

°C. The initial temperatures for thermal helium desorption were 740 and 640 °C for the specimens implanted at 400 or 600 °C, respectively and both of them were higher than the implantation temperatures. There was only one desorption peak ( 785 and 700 °C, respectively ) below 900 °C in both cases. The THDS results of the specimen after 8 keV He<sup>+</sup> implantation at 600 °C to a fluence of  $1 \times 10^{18}$  ions/cm<sup>2</sup> gives a desorption peak temperature of 700 °C<sup>[1]</sup> which is the same with the temperature in our study. The initial temperature for thermal helium desorption, the temperature at the peak, the desorption rate at the peak and the total desorption in the case of 400 °C were all higher than those in the case of 600 °C. No helium desorption observed for the specimen implanted at 800 °C.

SEM observation results after THDS test were shown in Fig. 2. Extensive exfoliation was observed, and the area of exfoliation increased with increasing implantation temperature from RT to 600 °C. Outside the exfoliation zones, small holes appeared for the RT case, while no holes for 400 and 600 °C cases. No significant surface modification after THDS test was observed for the specimen implanted at 800 °C.

The results indicated that helium desorption was detected for the specimens observed obvious surface modification. The diversity of surface modification for the RT specimen was in agreement with the multiple peaks, which indicated that helium release was controlled by different mechanism. The surface modification of only exfoliation for the 400 and 600 °C specimens was in agreement with the only one peak, which indicated helium release was controlled by one mechanism.

## Reference

- [1] Z. Fu, N. Yoshida, H. Iwakiri, Z. Y. Xu, J Nucl Mater, 329-33(2004)692.

## 3 - 9 Mechanical Properties Studies on High-energy Kr-ion Irradiated Corrosion Layer Fe<sub>3</sub>O<sub>4</sub>

Sun Jianrong, Song Peng, Zhang Hongpeng, Chang Hailong, Yao Cunfeng, Pang Lilong, Zhu Yabin, Cui Minghuan, Wang Ji, Zhu Huiping and Wang Zhiguang

The RAFM (Reduced Activation Ferritic/Martensitic) steel is considered as one of the promising candidate structural materials for LFRs (Lead alloy-cooled Fast Reactors) and ADS (Accelerator Driven Sub-critical system), and its compatibility with liquid metal and radiation-resistant properties have been extensively studied because of the requirements of reliability and safety of the blanket<sup>[1]</sup>. A number of corrosion experiments of RAFMs (Eurofer 97, T91 and 316L, *etc.*) in liquid LiPb alloy have been investigated, and the corrosion results show that these Fe-based steels suffered more serious corrosion attack from 480 to 550 °C, and the corrosion layer is made of the oxide layer (Fe<sub>3</sub>O<sub>4</sub> and Cr<sub>x</sub>Fe<sub>3-x</sub>O<sub>4</sub>) at steels' surface. Generally speaking, during the stage degeneration of material, the formation of corrosion layer is one of the important features of the process<sup>[2]</sup>. Cracking, blistering, embrittlement and other changes in materials may be induced by corrosion layers, and the corrosion layers have independent compositions, structures and radiation-resistant properties with distinguished from the alloy matrix. In a word, in order to further clarify the applicability of Fe-based structural materials in nuclear facilities, we should study not only the RAFM steel itself but also its corrosion layer (Fe<sub>3</sub>O<sub>4</sub>, mainly). So we report on modifications of mechanical properties of Fe<sub>3</sub>O<sub>4</sub> corrosion layer irradiated with high-energy ion.

The static corrosion experiments of T91 and RAFM steel specimens in liquid PbBi (Pb-44.5 at%) at 450 °C and irradiation experiment of Fe<sub>3</sub>O<sub>4</sub> at RT with 2.03 GeV Kr<sup>26+</sup> ions were performed in IMP (Institute of Modern Physics, Chinese Academy of Sciences, Lanzhou)<sup>[3]</sup>.

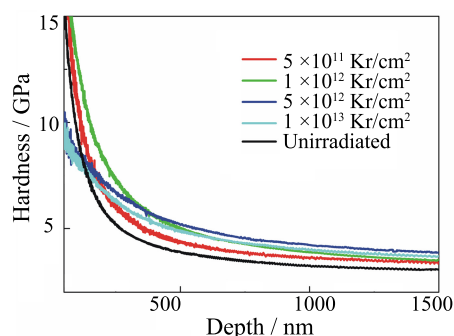


Fig. 1 (color online) Nano-hardness profiles of the unirradiated sample and the samples irradiated with different fluences at RT.

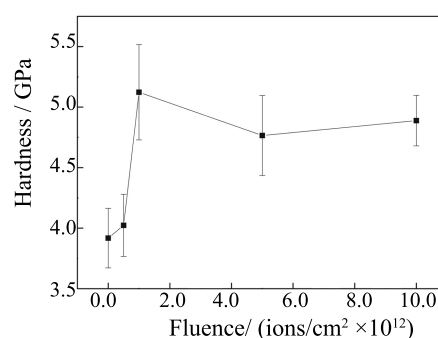


Fig. 2 (color online) The dependence of nano-hardness on the Kr<sup>26+</sup> ion fluence for Fe<sub>3</sub>O<sub>4</sub> films.

Fig. 1 shows the hardness variation of the pristine and irradiated  $\text{Fe}_3\text{O}_4$  films with depth from 0 to 1 500 nm. For the pristine film, the hardness declines from the maximum value of 34 GPa to a steady value of 3.9 GPa, indicating an indentation size effect. After irradiation, the films' hardness value increases slightly, but is not monotonic varying. In another words, the hardening and softening phenomena do exist for  $\text{Fe}_3\text{O}_4$  material induced by SHI irradiation. Fig. 2 shows the dependence of nano-hardness on the Kr-ion fluence for  $\text{Fe}_3\text{O}_4$  films. It is obviously, at low fluence level, as the formation of defects in the  $\text{Fe}_3\text{O}_4$  films induced by SHI irradiation, the value of nano-hardness increases slightly; and when the fluence increases from  $5.0 \times 10^{11}$  to  $1.0 \times 10^{12}$  ions/cm<sup>2</sup>, the value increases dramatically as the defects accumulation; after irradiation of  $1.0 \times 10^{12}$  Kr-ions/cm<sup>2</sup>, the value of nano hardness reaches to the maximum of 5.2 GPa, which is mainly because the number of grain boundaries increases significantly and acts as pinning sites of grain boundaries; when the irradiation fluences exceeds a certain value ( $1.0 \times 10^{12}$  Kr-ions/cm<sup>2</sup> for our work), the nano-hardness decreases consistently, which also can be explain that the annealing effect (relaxation) reduces the density and the size of vacancies, as a result of the numerous combinations of interstitials and vacancies. Though we can not confirm the type and distribution of the vacancy-type defects by our experiments, the changing regularities of magnetic and micro-mechanical properties of irradiated  $\text{Fe}_3\text{O}_4$  films shows excruciating uniform with different fluences, and they are significant correlation. In fact, the further measurement such as positron annihilation spectroscopy is carried out.

## References

- [1] A. R. Raffray, M. Akiba, V. Chuyanov, et al., J. Nucl. Mater, 307-311(2002)21.
- [2] A. K. Rivai, M. Takahashi, J. Nucl. Mater. 398(2010)139.
- [3] J. R. Sun, Z. G. Wang, H. P. Zhang, et. al., J. Nucl. Mater. 455(2014)685.

## 3 - 10 Swift Heavy Ion Induced Modification of Fe/Cu Multilayers

Wei Kongfang, Li Bingsheng, Zhu Yabin, Zhu Huiping, Gao Ning, Shen Tielong,  
Yao Cunfeng, Sun Jianrong, Pang Lilong, Cui Minghuan, Chang Hailong, Wang Ji,  
Wang Dong, Sheng Yanbin, Zhang Hongpeng, Wang Zhiguang and Gao Xing

When swift heavy ion (SHI) passes through metallic multilayers, the kinetic energy of the ion is mainly deposited to target electron subsystem (electronic energy loss, Se) by the inelastic collisions involving excitation and ionization of the target atoms, which could induce atomic displacements and modify the interfacial structure<sup>[1-6]</sup>. Therefore, through the study of the process of the interfacial atoms diffusion induced by SHI irradiation, we could explore the possible mechanism of atomic displacement induced by swift heavy ion irradiation.

Multilayers with structure of Si/[Fe(10 nm)/Cu(10 nm)]<sub>5</sub> (the subscript refers to layer number) were prepared by alternating depositions of pure iron (99.99% Fe) and copper (99.99% Cu) on cleaved Si(100) substrates by magnetron sputtering at room temperature (RT). Before irradiation experiments, the samples annealed at 300 degrees Celsius for 2 h. Then, the multilayers were irradiated at RT with 792 MeV Ar to  $1 \times 10^{12}$ ,  $1 \times 10^{13}$  and  $3.4 \times 10^{14}$  ions/cm<sup>2</sup>. These samples were characterized using depth profile analysis of Auger electron spectroscopy (AES) and transmission electron microscopy (TEM) respectively. Then the intermixing among the different layers of the samples induced by incident heavy ions were investigated systematically.

AES depth profiles of the as-deposited Si/[Fe(10 nm)/Cu(10 nm)]<sub>5</sub> multilayers, along with the samples irradiated at RT with 792 MeV Ar-ion, are shown in Fig. 1. The abscissa and the ordinate represent the sputter time and the Si, Fe, and Cu atomic concentrations (at.%), respectively. The interfaces of as-deposited multilayers were found not to be sharp, and rather wide interfacial region could be observed, whereas the layered structure also could be observed. After irradiation at  $1.0 \times 10^{12}$  and  $1.0 \times 10^{13}$  ions/cm<sup>2</sup>, for the Fe layer, the Fe concentration was higher and the Cu concentration was lower than those of the corresponding part of as-deposited samples; for the Cu layer, the Fe concentration was lower compared with that of the as-deposited samples, and the Cu concentration was higher, which indicates that a de-mixing between the Fe and the Cu layers occurs. But when the irradiation fluence was  $3.4 \times 10^{14}$  ions/cm<sup>2</sup>, the layered structure completely disappeared.

TEM images of Si/[Fe(10 nm)/Cu(10 nm)]<sub>5</sub> irradiated at room temperature by 792 MeV Ar-ion are shown in Fig. 2. For the as-deposited multilayers, the layered structure of the multilayers was not obvious. After irradiation at  $1.0 \times 10^{12}$  and  $1.0 \times 10^{13}$  ions/cm<sup>2</sup>, the layered structure could be observed. Up to a fluence of  $3.4 \times 10^{14}$  ions/cm<sup>2</sup>, the layered structure completely disappeared.